Systemic Therapy of Disseminated Myeloma in Passively Immunized Mice Using Measles Virus-infected Cell Carriers

Chunsheng Liu[1], Stephen J Russell[1] and Kah-Whye Peng[1]

[1]*Department of Molecular Medicine, Mayo Clinic, Rochester, Minnesota, USA*

Multiple myeloma (MM) is bone marrow plasma cell malignancy. A clinical trial utilizing intravenous administration of oncolytic measles virus (MV) encoding the human sodium-iodide symporter (MV-NIS) is ongoing in myeloma patients. However, intravenously administered MV-NIS is rapidly neutralized by antiviral antibodies. Because myeloma cell lines retain bone marrow tropism, they may be ideal as carriers for delivery of MV-NIS to myeloma deposits. A disseminated human myeloma (KAS 6/1) model was established. Biodistribution of MM1, a myeloma cell line, was determined after intravenous infusion. MM1 cells were found in the spine, femurs, and mandibles of tumor-bearing mice. Lethally irradiated MM1 cells remained susceptible to measles infection and transferred MV to KAS 6/1 cells in the presence of measles immune sera. Mice-bearing disseminated myeloma and passively immunized with measles immune serum were given MV-NIS or lethally irradiated MV-NIS-infected MM1 carriers. The antitumor activity of MV-NIS was evident only in measles naive mice and not in passively immunized mice. In contrast, survivals of both measles naive and immune mice were extended using MV-NIS-infected MM1 cell carriers. Hence, we demonstrate for the first time that systemically administered cells can serve as MV carriers and prolonged survival of mice with pre-existing antimeasles antibodies.

Received 24 November 2009; accepted 18 February 2010; published online 16 March 2010. doi:10.1038/mt.2010.43

INTRODUCTION

Multiple myeloma (MM) is an incurable malignancy of antibody secreting plasma cells that is disseminated predominately throughout the bone marrow as infiltrates or tumor nodules.[1] The American Cancer Society estimates that about 20,580 new cases of MM will be diagnosed in 2009 and about 10,000 Americans are expected to die of MM. Remission of newly diagnosed MM can be achieved with steroids, chemotherapy, thalidomide, bortezomib, and autologous stem cell transplantation.[2] However, the 5-year relative survival rate for MM is around 35% and for patients who relapse after primary therapy, outcomes are very poor. These individuals, as well as those who do not respond to initial therapy, have relapsed/refractory disease and are candidates for clinical trials testing combination drug therapy or investigational new drugs.[3]

One class of promising experimental targeted therapeutic is oncolytic viruses.[4–8] Targeted viral infection of tumor cells can cause direct cell destruction and/or elicit innate and cellular antitumor immune responses.[9–11] Attenuated measles virus (MV) has shown promise in preferential killing of tumor cells, particularly MM.[12–14] Cell entry of MV is initiated by binding of the measles hemagglutin glycoprotein to CD46 or signaling lymphocyte activating molecule receptors on the cell surface, and fusion triggering of viral-cell membranes via the fusion envelope glycoprotein. Expression of the measles hemagglutin and fusion proteins on infected cells results in the characteristic MV-induced cytopathic effect of syncytial formation.[12] MM cells express significantly higher numbers of CD46 receptors on the cell surface compared to the normal hematopoietic cells in the bone marrow.[15] As a result of the high CD46 expression, tumor cells are preferentially killed by oncolytic MV compared to nontransformed cells.[15,16] In addition, tumor-specific targeting can be achieved by attaching a single-chain antibody to retarget viral particles to myeloma specific receptors (e.g., CD38, Wue-1) on MM cell surface.[17–19] An engineered oncolytic MV encoding the human thyroidal sodium-iodide symporter (MV-NIS) is currently undergoing phase I clinical evaluation (intravenous administration) in patients with relapsed/refractory myeloma at Mayo Clinic (Rochester, MN). The NIS protein concentrates radioiodine and can be used in both isotopic imaging of gene transfer and radiovirotherapy of target tissues using β-emitting radioiodine to enhance therapeutic activity of the virus.[14,20,21]

There are, however, a number of challenges associated with intravenous administration of viruses that could limit the efficiency of measles virotherapy.[12] Intravenously injected MV can be quickly neutralized by antimeasles antibodies in previously vaccinated individuals.[22] Liver and spleen sequestration of viral particles also reduces the circulatory half-life of the virus and bioavailability to tumor cells (K.-W. Peng, unpublished data). In addition, the virus has to extravasate efficiently from the lumenal side of tumor blood vessels into the tumor parenchyma to initiate an infection. Indeed, these are generic issues that apply to systemic administration of viruses and/or vectors and various laboratories are developing innovative approaches to overcome these challenges.

Correspondence: *Kah-Whye Peng, Department of Molecular Medicine, Mayo Clinic, Guggenheim 18, 200 First Street SW, Rochester, Minnesota 55905, USA. E-mail: peng.kah@mayo.edu*

Using infected cells as virus carriers can potentially alleviate virus sequestration and neutralization by host immune factors.[23–25] Cells infected with replication-competent viruses can potentially serve as "Trojan horses" to deliver viruses to tumor sites, thus protecting viruses from neutralization by circulating antiviral antibodies. Indeed, MV may be particularly suited for cell carrier delivery as natural MV infection is cell-associated.[26] In this study, we explored the use of irradiated MM1 cells for delivery of MV-NIS to disseminated myeloma nodules in passively immunized mice. We showed that there were significantly higher numbers of MM cell carriers in the bone marrow of tumor-bearing mice compared to tumor-free mice. Lethally irradiated MM1 cells retained their ability to express MV genes, albeit to a lower level, heterofused with and transferred the MV infection to myeloma cells in the presence of antimeasles antibodies. The potential of virus-infected MM1 cells to extend the survival of measles immune mice-bearing disseminated myeloma disease was also determined.

RESULTS

Disseminated model of human MM in the SCID mouse

To establish a reproducible disseminated human KAS 6/1 MM model in the severe combined immunodeficiency (SCID) mouse, three pilot experiments (5–8 mice each time) were performed utilizing intravenous (tail vein) administration of KAS 6/1 cells. To facilitate noninvasive tracking of tumor location and tumor burden, KAS 6/1 cells were transduced with lentiviral vectors to express firefly luciferase (Fluc) and/or Gaussia luciferase (Gluc) and cyan fluorescent protein (CFP). Bioluminescent imaging of Fluc activity identifies the sites of tumor growth in the bone marrow, whereas levels of secreted Gluc in whole blood gives a quantitative measurement of tumor burden over time.[27,28] All three independent experiments showed a highly reproducible increase in tumor burden in mice over time (**Figure 1a**). Images from bioluminescent imaging indicated that the tumors engrafted and established predominantly in the spine, knee joints, and lower jaw bone (mandibles) by day 25 (**Figure 1b**). Fluorescence microcopy examination for CFP (**Figure 1c**) revealed that the KAS 6/1 tumors were located mainly in the spine (95%) typically at the thoracic and lower lumbar vertebral regions, hindlimbs (75%), ribs/sternum (85%), and lower jaw bone (65%). Mice typically develop hindlimbs paralysis and hunched postures (kyphotic) from days 35–55. At advanced stages, subcutaneous tumors can be found at the scapular region of the vertebrate and in the mandible bones (**Figure 1d**). X-rays of skeletons indicated osteolytic lesions in the spine and/or fractures at the femur or jaw bone due to tumor growth and erosion of the bone (**Figure 1d**), mirroring pathologies similar to the human disease.[29]

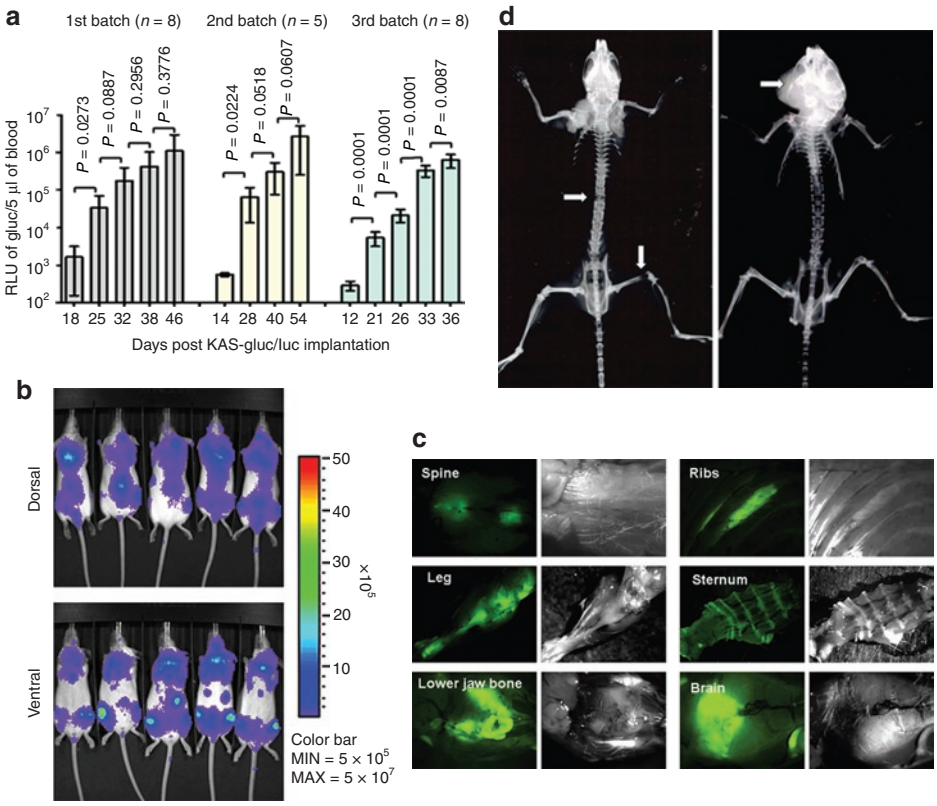

Figure 1 Characterization of the KAS 6/1 disseminated human multiple myeloma SCID mouse model. ICR-SCID mice were injected intravenously via the tail vein with 6×10^6 KAS 6/1-Gluc-CFP cells. (**a**) Tumor growth in mice from three independent experiments was monitored by measuring Gaussia luciferase (Gluc) activity in 5 µl of whole blood (n = 5–8 mice per batch). $P < 0.05$ denotes significant increase in tumor burden compared to the previous time point. (**b**) Bioluminescent imaging for firefly luciferase activity showing distribution of human myeloma disease in bone marrow of mice. (**c**) Images of explanted tissues showing presence of CFP^+ tumors predominantly in the spine, legs (femur), lower jaw bones (mandible). (**d**) X-ray images taken of the skeleton of mice with advanced myeloma disease indicate presence osteolytic lesions or fractures (white arrows) in the spine, legs, or mandible due to myeloma growth. CFP, cyan fluorescent protein; SCID, severe combined immunodeficiency.

Susceptibility of MM1 to MV infection after lethal irradiation and the safety for viral delivery

Since use of myeloma cells as carriers would require them to be lethally irradiated before infusion, MM1 cells were first irradiated with 5, 10, 20, or 40 Gy of ionizing radiation and then infected with MV-expressing green fluorescent protein (GFP) (MV-GFP) at multiplicities of infection (MOI) of 0.5, 1.0, or 2.0 (**Figure 2**). The numbers of GFP-expressing cells were determined 48 hours later using flow cytometry (**Figure 2b**). More than 90% of the 10 Gy irradiated MM1 cells (MOI of 1.0 or 2.0) were expressing GFP by 48 hours. However, the infection rate decreased to 50% in cells previously irradiated with 40 Gy. Cell viability and tumorigenicity of irradiated MM1 cells were determined using a clonogenic assay and tumorigenicity assay employing intravenous administration of cells into SCID mice. As shown in **Figure 2c**, irradiation at 5 Gy resulted in >95% reduction in clonogenicity of the MM1 cells. No colonies were found if cells had been irradiated with 10, 20, or 40 Gy ionizing irradiation. Mock irradiated or lethally irradiated MM1-Fluc cells in mice postintravenous administration was followed by bioluminescence imaging for Fluc activity (**Figure 2d**). In contrast to mice that received mock-irradiated MM1-Fluc cells, no bioluminescent signals (no tumor growth) were seen if MM1 cells had previously been irradiated with 10 Gy or 40 Gy. Mice in these groups survived long term and remained tumor free at 100-days postcell implantation (**Figure 2d**). For all subsequent experiment, MM1 cells were irradiated with 10 Gy (RT10) as these cells still support robust *MV* gene expression but have lost their clonogenicity and tumorigenicity.

Biodistribution of MM1 cell carrier in mice with disseminated KAS 6/1 myeloma disease

MM1 or KAS 6/1 cells were labeled with ^{111}Indium oxine and given intravenously to tumor-free control (CTL) mice or mice with disseminated KAS 6/1 disease (KAS). Both MM1 and KAS 6/1 myeloma cell lines have very similar biodistribution profiles in major organs of tumor-free CTL and tumor-bearing KAS mice (**Figure 3a**). SPECT-CT imaging and dosimetry data indicated that the majority of cell carriers arrested initially in the lungs (data not shown) and subsequently trafficked predominately to the liver (**Figure 3a**). These myeloma cells subsequently died because tumor nodules were not found in the liver at necropsy. About 5% of the injected dose was found in the kidneys at 24 hours postcell administration, likely as a result of isotope release from nonviable cells. To determine whether cell carriers accumulated in the bone marrow of mice, major organs were dissected and removed from the mice and the carcasses were then imaged using a gamma camera (**Figure 3b**). Planar gamma camera imaging showed higher levels of ^{111}Indium activity in the skeleton of the KAS 6/1 tumor-bearing animal than in the tumor-free control mouse (**Figure 3b**). Analysis of the head region showed a large CFP$^+$ tumor nodule in the lower jaw bone, which corresponded to the higher radioactive signal in the head region of the planar gamma camera image (**Figure 3b**). Since myeloma cells have a tropism for

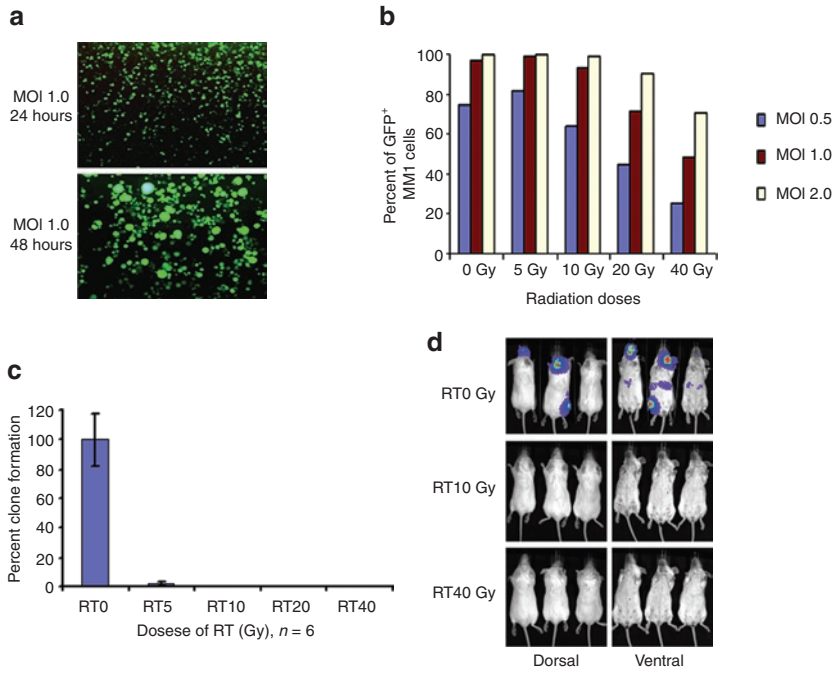

Figure 2 Feasibility of lethally irradiated MM1 cells as a vehicle for MV delivery. (**a**) 10 Gy lethally irradiated MM1 cells remained susceptible to MV-GFP infection and expressed viral proteins, resulting in syncytia formation 48 hours postinfection. (**b**) Quantitation of viral infection and expression in irradiated cells by measuring percentage of single cells expressing GFP using flow cytometry. (**c**) Clonogenic assays showed that irradiation (RT) resulted in significant loss of MM1 cell viability and clonogenicity at 14 days after cell plating (n = 6 replicates per RT condition). RT0, mock irradiated. (**d**) Bioluminescent images showing tumor growth in mice injected intravenously with nonirradiated (RT0 Gy) MM1-Fluc cells. In contrast, no tumor growth was seen in mice given lethally irradiated (RT10 or RT40 Gy) MM1-Fluc cells at 42 days after cell infusion. Fluc, firefly luciferase; GFP, green fluorescent protein; MM, multiple myeloma; MOI, multiplicities of infection; MV, measles virus.

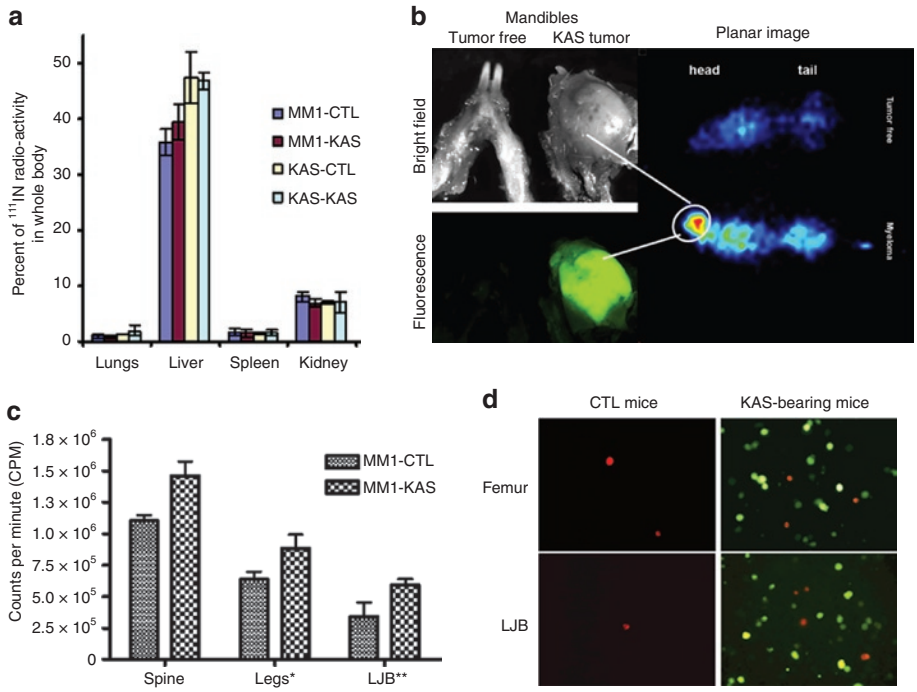

Figure 3 Biodistribution of MM1 cell carriers after intravenous delivery in SCID mice-bearing disseminated KAS 6/1 myeloma disease. (**a**) Percentage of ^{111}Indium oxine-labeled MM1 or KAS 6/1 cells in organs harvested from tumor-free SCID mice (CTL) or mice with disseminated KAS 6/1 disease (KAS). (**b**) Whole body planar gamma camera image of tumor free or tumor-bearing mice given ^{111}Indium oxine-labeled MM1 cells. The hot spot in the gamma camera image (circled) correlated with the presence of a large CFP$^+$ KAS 6/1 tumor in the mandible. (**c**) Dosimetry measurements (counts per minute) showing the amount of radiolabeled MM1 cells in a portion of the spine, legs, or mandibles of KAS 6/1-bearing mice as compared to normal control (CTL) mice. (**d**) Fluorescence microscopy confirmed presence of DiI-labeled (red) MM1 cells in the bone marrow flushings obtained from the femurs and lower jaw bones (LBJ) of tumor free and KAS 6/1 (CFP$^+$)-bearing mice. CFP, cyan fluorescent protein; IN, indium; MM, multiple myeloma; SCID, SCID, severe combined immunodeficiency.

the bone marrow, equivalent portions of the spine, leg (femur), and lower jaw bones of mice given ^{111}Indium oxine-labeled MM1 cell carriers were harvested and the amount of radioactivity was quantitated (**Figure 3c**). A higher level of radioactivity, indicating higher numbers of ^{111}In labeled MM1 cell carriers, was measured in the bones harvested from KAS 6/1 tumor-bearing mice compared to tumor-free CTL mice (**Figure 3c**). DiI-labeled MM1 (red) cells were also more readily detected by fluorescence microscopic analysis of bone marrows flushed from the femurs and lower jaw bones of KAS 6/1 mice than tumor-free CTL mice (**Figure 3d**).

In vitro transfer of MV infection from MM1 cell carrier to target cells

The ability of MV-Luc-infected MM1 carrier cells to transfer the virus to KAS 6/1 myeloma target cells was assessed in a coculture experiment (**Figure 4**). MM1 cells [labeled green with CellTracker Green CMFDA (Invitrogen, Eugene, OR)] were preinfected with MV-Luc and 18 hours later, were mixed with KAS 6/1 cells (labeled red with CellTracker CMPTX) at 1:1 ratio. At 2 hours after mixing the cells remained as single cells and no fusion events were seen (**Figure 4a**). At 48 hours and 72 hours after coculture, significant heterocellular fusion was observed between the red MM1 cells and green KAS 6/1 cells to result in large syncytia (**Figure 4c**). In contrast, no heterofusion events were seen if uninfected MM1 cells were mixed with KAS 6/1 cells (**Figure 4d**). It is also important to note that the extent of cell fusion using 10 Gy irradiated infected MM1 cells was comparable to that with nonirradiated MM1 cells (**Figure 5a**). The amount of MV progeny produced by 10 Gy irradiated MV infected MM1 was examined in one step growth curve (**Figure 5b**). Cell-associated virus titer peaked at 48 hours postinfection, confirming that lethally irradiated MM1 cells were still able to propagate the virus.

MM1 cell carrier protects MV-NIS from neutralizing antimeasles antibodies

MV-NIS infected 10 Gy irradiated MM1 cell carriers were added to a monolayer of Vero cells in the presence of increasing amounts of measles immune human sera [diluted 1:8 to 1:256, corresponding to 37.4 to 1.15 EU/ml of anti-MV immunoglobulin G (IgG)] for 2 days. The numbers of plaques (syncytia) formed as a result of virus transfer from infected MM1 cells to Vero cells were counted. As shown in **Figure 5c**, the numbers of infection/heterofusion events decreased with increasing amounts of measles immune sera. However, it is also evident that cell-associated viruses are more resistant to antimeasles antibodies; MM1-mediated virus transfer occurred at 37.4 EU/ml compared whereas cell-free MV-NIS was able to initiate infection only at 4.7 EU/ml.

The observation that cell carriers are superior at delivering MV in the presence of antimeasles antibodies was also demonstrated in a cell killing assay where KAS 6/1-Fluc cells were incubated with MV-NIS (**Figure 6a**) or MV-NIS infected nonirradiated, 10 Gy irradiated (RT10) ,or 40 Gy irradiated (RT40) MM1 cell carriers in the presence of measles immune serum. MV-NIS infected RT10-MM1 and nonirradiated MM1 cells exhibited similar killing effect

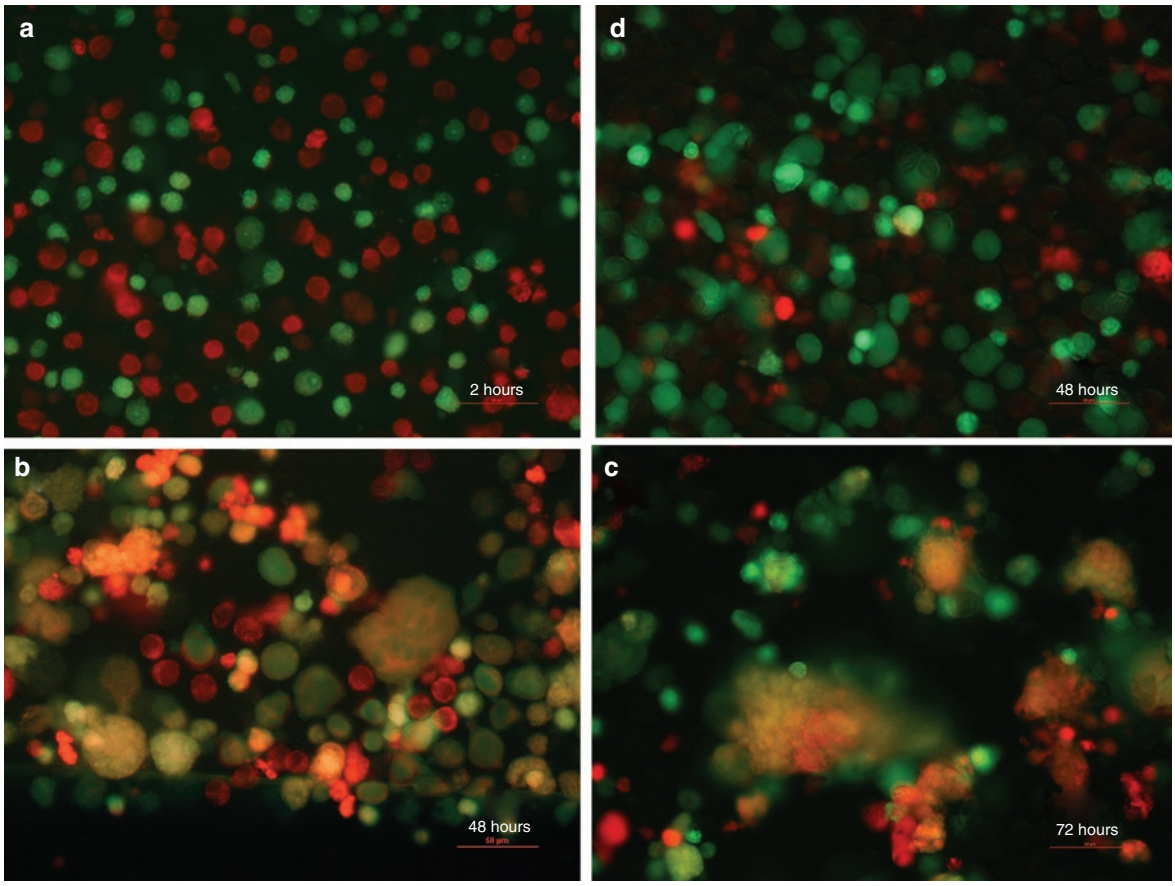

Figure 4 High-resolution analysis of heterofusion between green MM1 and red KAS 6/1 cells which resulted in observation of dual colored syncytia. At 18 hours postinfection, MV-Luc infected (MOI 1.0) MM1 cells (labeled green with CellTracker Green CMFDA) were mixed with KAS 6/1 target cells (labeled red with CellTracker Red CMPTX) at a 1:1 ratio. At (**a**) 2 hours, (**b**) 48 hours, and (**c**) 72 hours after mixing, the cells were photographed using a fluorescence microscope at (original magnification ×200) under blue and green light separately and the photographs were merged, yielding "orange colored" syncytia. (**d**) Coculture of uninfected MM1 cells (green) with KAS 6/1 cells (red) did not result in heterofusion of cells or syncytia. Bars = 50 µm. MM, multiple myeloma; MOI, multiplicities of infection; MV, measles virus.

on the KAS 6/1-Fluc cells as indicated by decrease in Fluc activities (Figure 6b,c). In contrast, cell-free MV-NIS failed to exert its neoplastic cell killing activity due to virus neutralization by antimeasles antibodies (Figure 6a). We also noted that the extent of cell killing induced by irradiated cells was lower than nonirradiated cells (Figure 6c,d). In particular, MV-NIS infected MM1 cells irradiated with 40 Gy were unable to induce significant cell killing at 18.7 EU/ml and were only partially effective at 9.4 EU/ml (Figure 6d). Hence, for all subsequent experiments, we chose to irradiate the cell carriers at 10 Gy which was sufficient to induce total loss in cell clonogenicity and tumorigenicity (Figure 2c,d).

Systemic delivery and treatment outcomes using virus-infected MM1 cell carriers

Before loading with MV-NIS, MM1 cell carriers received 10 Gy ionizing radiation (RT10-MM1) and were then incubated with MV-NIS for 2 hours. Cells were then maintained in standard culture conditions overnight. The MV-NIS infected RT10-MM1 cell carriers or cell-free MV-NIS were used to treat measles naive or passively immunized SCID mice-bearing disseminated KAS 6/1 tumors. The establishment and progression of disseminated myeloma disease in these mice was monitored using bioluminescent imaging for Fluc-expressing KAS 6/1 cells. As shown in Figure 7a,b, KAS 6/1 tumors were apparent in the knee joints and spine of mice at day 27 post IV administration of tumor cells. Three hours pretherapy, some animals received an intraperitoneal injection of saline whereas others were passively immunized by intraperitoneal injection of measles immune human serum (anti-MV IgG titer = 40 EU per mouse). Animals were then treated IV with saline, MV-NIS (3×10^6 $TCID_{50}$) or MV-NIS infected RT10-MM1 cells (3×10^6 cells). Bioluminescent images and quantitation of Fluc activity (photon counts) indicated that disseminated myeloma disease developed progressively in saline treated animals, resulting in a significant increase in tumor burden by day 41 (Figure 7). In contrast, MV-NIS significantly suppressed tumor progression and resulted in effective control of myeloma disease, but only in measles naive mice and not in measles immune mice. On the other hand, treatment of both measles naive and measles immune mice with MV-NIS infected RT10-MM1 cells achieved good tumor control (Figure 7).

The long-term survivals of mice in the various treatment groups were plotted in a Kaplan–Meier curve. As shown in Figure 7c, median survival was 45 days in the saline-treated group, 50 days in MV-NIS (+Ab) group, 72 days in MV-NIS (−Ab)

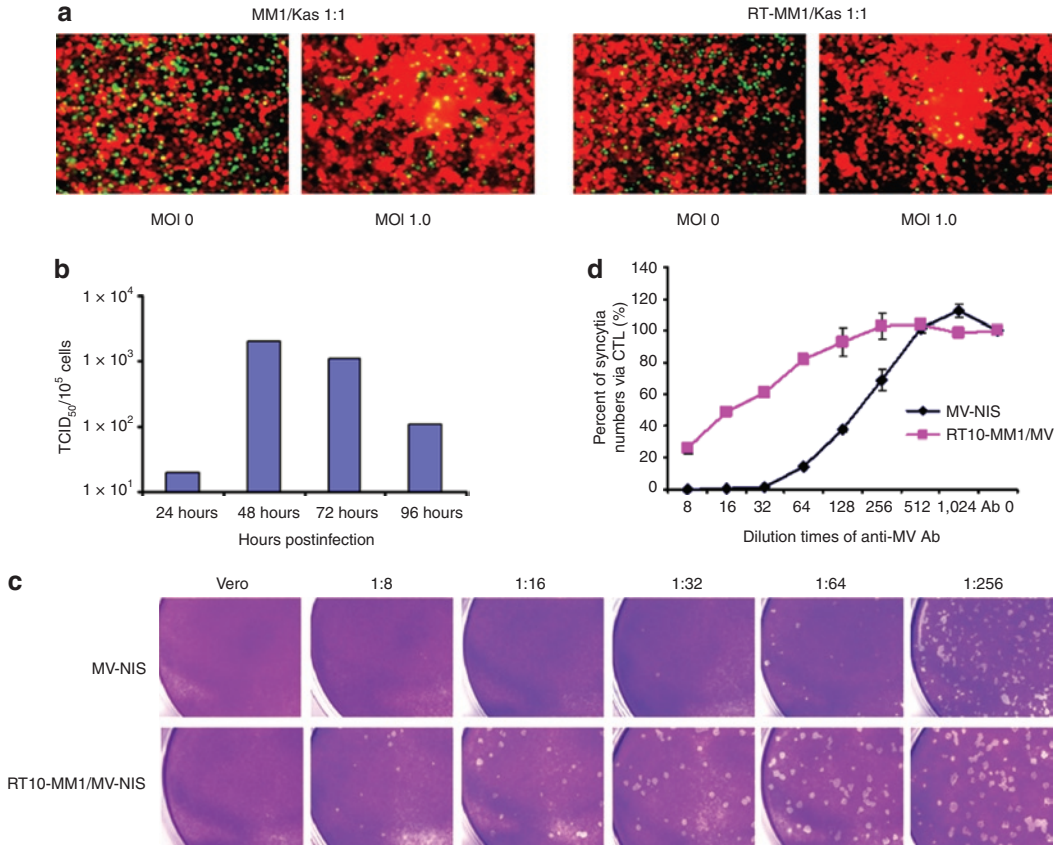

Figure 5 Transfer of MV-NIS infection from irradiated MM1 cell carriers to target cells in the presence of antimeasles antibodies. (**a**) Coculture of CMFDA green labeled nonirradiated or 10 Gy irradiated MM1 cells with DsRed-expressing KAS 6/1 cells. Extensive cell fusion was observed between MV-NIS infected RT-MM1 cells (MOI 1.0) and KAS 6/1 cells after 48 hours of coculture. (**b**) Production of MV progeny in RT10-MM1 cells over time. Cell-associated virus titer peaked at 48 hours postinfection. (**c**) Crystal violet staining for syncytia in Vero cell monolayer at 48 hours postinfection with cell-free MV-NIS or cocultured with MV-NIS infected RT10-MM1 cells in the presence of increasing dilutions of measles immune sera. (**d**) Quantitation of the numbers of syncytia induced by MV-NIS or cell-associated virus (RT10-MM1/MV) in the Vero monolayer in the absence (Ab 0) or presence of measles immune sera (dilution 1:8 to 1:1,024). MM, multiple myeloma; MOI, multiplicities of infection; MV, measles virus.

group, 60 days in MV-NIS/RT10-MM1 (+Ab) group, and 65 days in MV-NIS/RT10-MM (−Ab) group. In addition, about 20, 30, and 40% of mice survived >100 days in the MV-NIS/RT10-MM1 (+Ab) group, MV-NIS/RT10-MM1 (−Ab) group, and MV-NIS (−Ab) group, respectively. The P values comparing survival curves for saline treated versus MV-NIS (+Ab) is <0.005; saline versus MV-NIS/RT10-MM1 (+Ab) is $P < 0.0001$; MV-NIS (−Ab) versus MV-NIS/RT10-MM1 (−Ab) $P > 0.1$; MV-NIS (−Ab) versus MV-NIS (+Ab) $P < 0.0001$, MV-NIS/RT10-MM1 (−Ab) versus MV-NIS/RT10-MM1 (+Ab) $P > 0.5$.

DISCUSSION

MM is an incurable disseminated malignancy of plasma cells.[1] These neoplastic plasma cells can either be diffusely dispersed among the normal bone marrow cells (bone marrow-resident) or located in discrete, well-vascularized solid tumors (plasmacytomas) that may originate in bone or soft tissue. Myeloma causes debilitating osteolytic bone disease as a result of overactive osteoclastic activity and minimal osteoblastic activity in the tumor microenvironment. Patients experience bone pain, pathologic fractures, and hypocalcaemia.[29] In this study, we have developed a highly reproducible model of disseminated human myeloma in SCID mice where the sites of tumor growth can be imaged using bioluminescent imaging for Fluc activity and tumor burden can be quantitated by measurement of levels of secreted Gluc activity in the blood of mice. Using this model, we evaluated the feasibility of using a lethally irradiated myeloma cell line to deliver oncolytic MV to myeloma deposits in measles immune mice.

There are several compelling reasons to use cell carriers for systemic delivery of an oncolytic virus. Unlike "naked" MV which can be rapidly sequestered by the reticuloendothelial system or neutralized by antiviral antibodies in the circulation, we have demonstrated here that cell-associated MVs are protected from antiviral antibodies. Subsequent virus transfer via heterocellular fusion between infected cell carriers with target cells is more resistant to neutralization by antimeasles, perhaps because the interface of cell-to-cell fusion is less accessible to antibodies than the junction of virus-cell membrane fusion. However, another set of challenges is associated with use of cells as carriers for virotherapy. Many studies have shown that systemically administered cell carriers tend to arrest in the lungs immediately upon infusion.[25,30–32] We have previously demonstrated that CD14 monocytes, immature dendritic cells, interleukin-2 expanded T cells and, in this study, irradiated MM1 cells arrested in lungs of the mice and

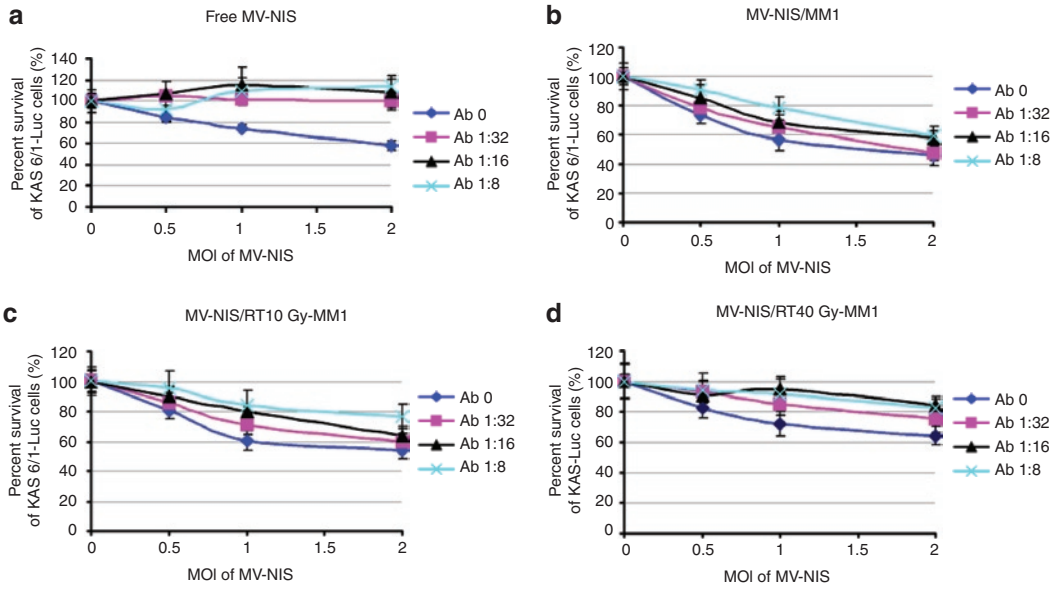

Figure 6 KAS 6/1 cell killing by MV-NIS or MM1 cell-associated MV-NIS in the presence of antimeasles antibodies. (**a**) KAS 6/1 cells stably expressing Fluc cells were infected with MV-NIS or cocultured with MV-NIS infected, (**b**) nonirradiated MM1, (**c**) 10 Gy irradiated, or (**d**) 40 Gy irradiated MM1 cells. Various multiplicities of infection (MOI) of MV-NIS were tested. Cell killing was measured by quantitation of firefly luciferase activity in viable KAS 6/1-Fluc cells at 48 hours after mixing. Fluc, firefly luciferase; MM, multiple myeloma; MV, measles virus.

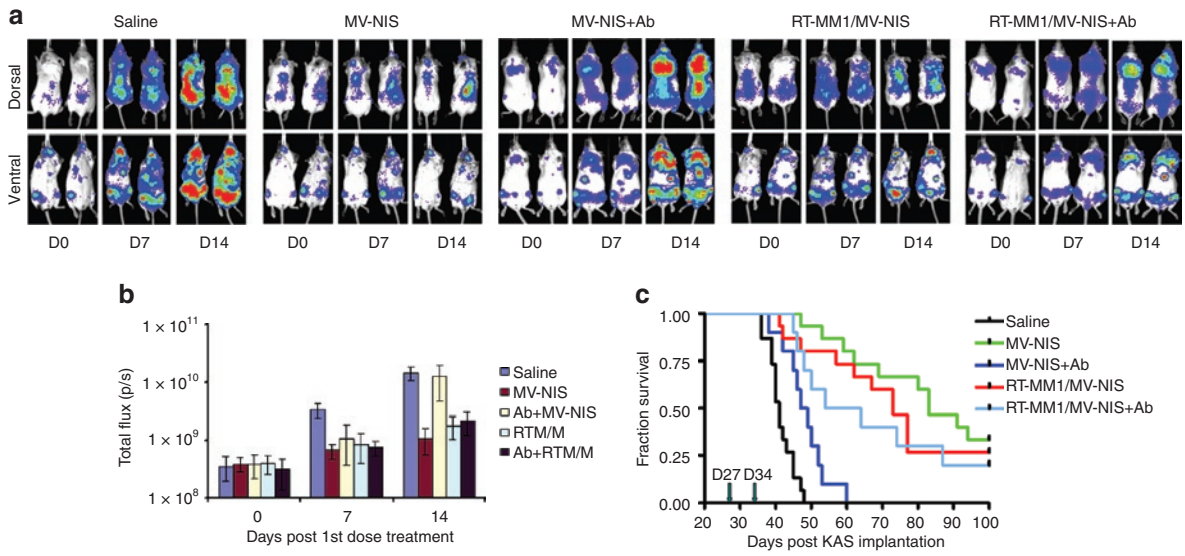

Figure 7 Systemic delivery and treatment outcome using MV-NIS infected RT10-MM1 cell carries in measles naive and passively immunized SCID mice-bearing disseminated KAS 6/1 myeloma disease. (**a**) Bioluminescent images showing amount and location of myeloma disease in mice over time. (**b**) Quantitation of Fluc activity as a measurement of disease burden, and (**c**) Kaplan–Meier survival curves of mice in the various treatment groups. Fluc, firefly luciferase; MM, multiple myeloma; MV, measles virus; SCID, severe combined immunodeficiency.

later disseminated to the liver, spleen, and bone marrow after the initial arrest.[22,33] ^{111}Indium labeling studies here indicated that 2–5% of injected cells do arrive in the bone marrows of the spine or femur of mice. The pattern of transient cell arrest in the lungs and subsequent redistribution to liver and spleen is also seen in human studies where ^{111}Indium oxine-labeled peripheral blood lymphocytes or T cells were injected intravenously into humans and monitored using gamma cameras.[34,35] Indeed, the feasibility of intravenous cell delivery has been validated by numerous clinical studies using adoptive transfer of *in vitro* expanded T cells for immunotherapy of cancer, utilizing doses as high as 5×10^{10} cells per patient.[36,37]

The attractive feature of using a myeloma cell line such as MM1 as a carrier for myeloma therapy is that circulating myeloma cells can home to the bone marrow in response to cytokines produced by bone marrow stromal cells. The trafficking profiles of myeloma cells are well studied.[38,39] Myeloma cells are malignant plasma cells programmed to home to the bone marrow where they are committed to differentiate in close association with the bone marrow microenvironment. Bone marrow homing of myeloma

cells is mediated by a multistep process of extravasation starting with adhesion to the vascular endothelium, invasion of the subendothelial basement membrane, followed by further migration within the stroma, mediated by chemotactic factors.[38] At advanced stages of myeloma disease, these malignant plasma cells develop autocrine growth supporting loops that enable them to survive and proliferate in the absence of the bone marrow microenvironment and to become stroma-independent.[38] The stimulus for bone marrow homing is mainly due to CXCR4 expression on myeloma cells that allow them to respond to CXCL12 or stromal cell derived factor-1α produced by bone marrow stromal elements.[40,41] After myeloma cells home to the marrow, they adhere to bone marrow stromal cells through binding of vascular cell adhesion molecule-1 on stromal cells and α4β1 integrin on myeloma cells.[29] The physical interaction involving various adhesion molecules between the myeloma cells and the stromal elements play an important role in myeloma disease. In particular, myeloma is highly vascularized and the density of the neovessel is proportional to plasma cell labeling index and increase with myeloma stage, providing a strong prognostic value.[42] Indeed, we can potentially exploit this high-microvessel density in myeloma deposits as a way to enhance virus or cellular localization through use of vascular binding ligands.[43]

In addition to its natural tropism for the bone marrow, the MM1 myeloma cells can efficiently be infected by MV as well as support viral gene expression even after lethal irradiation. The MM1 cells offer the convenience of a cell line that can be rendered good manufacturing practice grade and validated to meet release criteria suitable for human use. Per US Food and Drug Administration regulations, cell lines used in human studies will have to be lethally irradiated to ensure that they are not proliferative and incapable of establishing tumors.[44] A side effect from irradiation is that these irradiated MM1 cells generally have lower levels of viral gene expression, although these lethally irradiated myeloma cells can still be infected to nearly 100%, survive for a limited period of time to transfer the virus, are not clonogenic in agar colony forming assays or tumorigenic in SCID mice. However, a thorough safety study using high numbers of irradiated MM1 cell carriers in SCID mice should be performed as part of the toxicology studies before clinical testing of this therapy in humans. Precedence in using cells for therapy has been set in that numerous tumor vaccination studies are already using lethally irradiated single or a cocktail of gene-modified allogeneic tumor cell lines or autologous tumor cells.[44–46] Lethally irradiated Tall-104 cells, a cytotoxic T cell line have also been used in US Food and Drug Administration approved trials as a systemic infusion for treatment of patients with metastatic breast cancer.[47,48] The human experience in addition with the extensive toxicology and pharmacology studies have demonstrated the safety of using such lethally irradiated cell lines in patients with end stage cancer, making the strategy of cell carriers highly feasible for clinical testing.

We have previously determined that the average anti-MV IgG titers in myeloma patients (~36 EU/ml, $n = 10$), although many of these patients do not have detectable levels of anti-MV IgG (<20 EU/ml) due to their disease. These anti-MV IgG levels are much lower than that of healthy individuals (anti-MV IgG titers of ~100 EU/ml).[49] The antibody titer used in the therapy experiment was set to 40 EU per mouse (~20 EU/ml) to mirror the biological concentration of anti-MV IgG in myeloma patients. Although many reports have elegantly shown the feasibility of cell carriers for virus delivery to a variety of tumor xenografts, we demonstrate here for the first time, that systemic administration of a virus-infected cell carrier can significantly extended the survival of passively immunized mice-bearing disseminated human myeloma disease and overcome pre-existing antibodies. In contrast, the antitumor activity of the naked virus in these immune mice was negated by the presence of pre-existing antibodies. Based on these findings, we are encouraged to pursue virus-infected MM1 cell carriers for delivery of viruses in patients with disseminated MM.

MATERIALS AND METHODS

Cell culture and animals. Vero cells purchased from the American Type Culture Collection (Manassas, VA) were cultured in Dulbecco's modified Eagle's medium supplemented with 5% fetal bovine serum, 100 μg/ml penicillin, and 100 μg/ml of streptomycin. MM1 and KAS 6/1 (kind gifts from R. Fonseca and D.F. Jelinek, Mayo Clinic, Rochester, MN) were cultured in 10% RPMI-1640. Medium for KAS 6/1 cells was supplemented with 1 ng/ml recombinant human interleukin-6 (R&D Systems, Minneapolis, MN). Four to six-week-old female ICR-SCID mice were purchased from Taconic (Germantown, NY). All animal experiments were reviewed and approved by the Institutional Animal Care and Use Committee.

Lentivectors and transduction of myeloma cells. To generate the lentivectors, gag-pol expression plasmid pCMVΔ8.91, VSV.G envelope expression plasmid pMD-G, and Fluc expression vector plasmid pHR′-SIN-Fluc[50] or Gluc expression vector plasmid pCSCW-Gluc-IRES-CFP[51] were cotransfected into 293T cells. The supernatant was collected 48 hours after transfection, filtered (0.45 μm) and frozen at –80 °C until use. KAS 6/1 cells expressing Gluc, CFP and/or Fluc and KAS 6/1-DsRed cells were generated by transduction of KAS 6/1 cells using lentiviral vectors expressing Gluc-cyan fluorescence protein or Fluc or DsRed fluorescent protein.

MV propagation, titration, and infection. The construction, characterization, and $TCID_{50}$ titration method for MV encoding the human thyroidal sodium-iodide symporter (MV-NIS), MV-expressing Fluc (MV-Fluc), measles-expressing green fluorescence protein (MV-GFP) have been described previously.[14,22,52] For infection assays, viruses were mixed with 500 μl of target cell suspension in reduced serum media Opti-MEM at different MOIs (0, 0.5, 1.0) and incubated at 37 °C for 2–3 hours. The virus inoculum was removed and cells were maintained in appropriate growth media at 37 °C.

Determination of MV infection rate by flow cytometric analysis. After 5, 10, 20, or 40 Gy irradiation using a ^{137}Cs source, MM1 cells were infected with MV-GFP at MOI of 0.5, 1.0, or 2.0 for 24, 48, and 72 hours. The infection rate was determined by both flow cytometric analysis and fluorescence microscopy. For flow cytometric analysis analysis, 40 μg/ml of a fusion inhibitory peptide was used to inhibit intercellular fusion to enable quantitation of single GFP-expressing cells.

Clonogenic assay. In order to find out the lethal irradiation dose for MM1, a clonogenic assay was employed. MM1 cells were irradiated at 5, 10, 20, or 40 Gy in 0.5 ml of growth medium (1,000 cells/ml) and cells were added to 2.5-ml methylcellulose base medium (R&D Systems) and plated into a 35-mm dish at a density of 500 cells/dish. Fourteen days later, the numbers of MM1 colonies (>50 cells) per treatment group was counted. The final result was an average of triplicates repeated in two different experiments.

In vitro *antimeasles antibody test and crystal violet staining.* Vero cells were plated overnight in 6-well plates (2×10^5 cells/well). The next day, 2,000

$TCID_{50}$ of MV-NIS or 2,000 MV-NIS infected MM1 cells (MOI 1.0) were added to the adherent Vero cell monolayer in the presence of serially diluted measles immune human AB serum (anti-MV IgG titer = 300 EU/ml; Valley Biomedical, Winchester, VA). Forty-eight hours later, cells were fixed with 0.5% glutaraldehyde and stained with 2% crystal violet, and the numbers of plaques (syncytia) were counted under light microscopy.

Cell heterofusion assay. Nonirradiated or 10 Gy irradiated MM1 cells were infected with MV-Luc or MV-NIS at MOI of 0.5, 1.0, or 2.0 and then were labeled with CellTracker Green CMFDA (Invitrogen). After mixing with CellTracker Red CMPTX labeled or DsRed-expressing KAS 6/1 target cells, the cell culture was maintained at 37 °C and the subsequent cell heterofusion was examined under fluorescence microscopy at 24, 48, 72, and 96 hours.

Fluc activity assay. Nonirradiated or 10 Gy irradiated MM1 cells were infected with MV-NIS at MOI of 0.5, 1.0, or 2.0. The next day, MV-NIS virus or MV-NIS-infected MM1 cells were mixed with KAS 6/1-Fluc cells in the presence of serially diluted measles immune human serum. The killing of Fluc-expressing KAS 6/1 by MV-NIS transfer from MM1 cells or MV-NIS infection was measured by determining Fluc activity. The Fluc activity was assayed at 24, 48, 72, and 96 hours and measured with Top Count NXT Scintillation and Luminescence Counter (Packard, Meriden, CT) in black 96-well plates at wavelength of 400–620 nm.

SPECT-CT scan and dosimetry measurements of ^{111}Indium labeled MM1 and KAS 6/1 cells in mice. In order to track the *in vivo* biodistribution of myeloma cells, 3×10^6 of MM1 or KAS 6/1 cells were labeled with 200 μCi ^{111}Indium oxine and Vybrant DiI (Invitrogen) and injected intravenously to tumor-free ICR-SCID mice or ICR-SCID mice-bearing disseminated KAS 6/1 disease. Twenty-four hours later, mice were anesthetized via isoflurane inhalation and imaged using a micro SPECT-CT machine (X-SPECT; Gamma Medica, Northridge, CA). After SPECT-CT or planar gamma camera imaging on the X-SPECT machine, radioactivity in the whole mouse, dissected major organs or equivalent portions of bones were measured using a Radioisotope Calibrator CRC-7 (Capintec, Ramsey, NJ) or the 1480 WIZARD 3″ Automatic Gamma Counter (Perkin-Elmer, Waltham, MA). The percentage of radioactivity per organ was calculated as a percentage of the whole animal. The presence of DiI-labeled MM1 cells was also evaluated using fluorescence microscopy after flushing the bone marrow of femurs or mandibles of mice. Another independent experiment was also performed for evaluation of MM1 distribution using bioluminescence imaging on the Xenogen IVIS 200 System (Caliper Life Sciences, Alameda, CA).[22]

Establishment of the disseminated KAS 6/1 human myeloma model in SCID mice. ICR-SCID mice were given whole body irradiation (2 Gy) 24 hours before intravenous tail vein injection of KAS 6/1 cells stably expressing Gluc and CFP (6×10^6 cells/100 μl). Tumor distribution and tumor burden were monitored respectively by noninvasive imaging for bioluminescent activity (Fluc expression) on the Xenogen machine and blood sampling to measure Gluc activity weekly.[28] Briefly, 5 μl of tail vein blood sample was taken and the activity of Gluc was measured using a Gluc assay kit (New England Biolabs, Ipswich, MA) and Top Count NXT Scintillation and Luminescence Counter (Packard) in a black 96-well plate at wavelength of 470 nm.

Therapy of measles naive or passively immunized mice using MV-NIS or infected cell carriers. Tumor burden in mice was quantitated by measuring Gluc activity and mice with Gluc activity between 10,000 and 50,000 RLU/5 μl blood were selected for randomization and use, whereas mice with Gluc activity <10,000 RLU/5 μl blood were not used in the experiment due to low-tumor burden. In the therapy experiment, 65 of 80 KAS 6/1-Gluc-CFP injected mice were selected and randomized into five groups: (i) placebo group (n = 15) was treated with 150 μl saline only; (ii) MV-NIS free-virus group (n = 15) was injected intravenously with 3×10^6 $TCID_{50}$ MV-NIS /150 μl; (iii) RT10-MM1/MV-NIS group (n = 15) was injected with 150 μl of MV-NIS infected (MOI 1.0) RT10-MM1 cell suspension (3×10^6 cells); (iv) Ab + MV-NIS group (n = 10) was passively immunized with intraperitoneal administration of 40 EU of anti-MV IgG 4 hours before MV-NIS; (v) Ab + RT10-MM1/MV-NIS group (n = 10) was pretreated with 40 EU anti-MV IgG 4 hours before RT10-MM1/MV-NIS injection. The concentration of 40 EU was equivalent to at 1:16–1:32 dilution of the antisera in the *in vitro* experiments. All mice were treated with two doses of the given therapy, including boosting with antisera. Mice were observed daily and were euthanized sacrificed when at least one of the following signs was observed: paralysis, head drop, inactivity, or weight loss >20%. All mice surviving at day 100 were euthanized at the end of the study. Necropsy was performed and tumor location and tumor burden were noted by examining the CFP expression in the major bones and organs including sternum, spine, ribs, lower jaw bone, legs, brain, liver, and lungs. Kaplan–Meier survival curves were generated to evaluate the treatments outcomes.

ACKNOWLEDGMENTS

We are grateful to the Alliance for Cancer Gene Therapy and the National Cancer Institute (CA100634, CA129966, and CA129193) for funding support. K.-W.P., S.J.R., and Mayo Clinic have a financial interest associated with technology used in this research. Patents have been awarded for this technology. They have been licensed to NISCO International, Inc. and Mayo Clinic holds an equity position in that company. No royalties have accrued to K.-W.P and S.J.R. or Mayo Clinic to date.

REFERENCES

1. Kyle, RA and Rajkumar, SV (2009). Treatment of multiple myeloma: a comprehensive review. *Clin Lymphoma Myeloma* **9**: 278–288.
2. Rajkumar, SV and Kyle, RA (2005). Multiple myeloma: diagnosis and treatment. *Mayo Clin Proc* **80**: 1371–1382.
3. Dingli, D and Rajkumar, SV (2009). Emerging therapies for multiple myeloma. *Oncology (Williston Park, NY)* **23**: 407–415.
4. Parato, KA, Lichty, BD and Bell, JC (2009). Diplomatic immunity: turning a foe into an ally. *Curr Opin Mol Ther* **11**: 13–21.
5. Nguyen, TL, Tumilasci, VF, Singhroy, D, Arguello, M and Hiscott, J (2009). The emergence of combinatorial strategies in the development of RNA oncolytic virus therapies. *Cell Microbiol* **11**: 889–897.
6. Stief, AE and McCart, JA (2008). Oncolytic virotherapy for multiple myeloma. *Expert Opin Biol Ther* **8**: 463–473.
7. Liu, TC, Galanis, E and Kirn, D (2007). Clinical trial results with oncolytic virotherapy: a century of promise, a decade of progress. *Nat Clin Pract Oncol* **4**: 101–117.
8. Kumar, S, Gao, L, Yeagy, B and Reid, T (2008). Virus combinations and chemotherapy for the treatment of human cancers. *Curr Opin Mol Ther* **10**: 371–379.
9. Chiocca, EA (2008). The host response to cancer virotherapy. *Curr Opin Mol Ther* **10**: 38–45.
10. Prestwich, RJ, Errington, F, Diaz, RM, Pandha, HS, Harrington, KJ, Melcher, AA *et al.* (2009). The case of oncolytic viruses versus the immune system: waiting on the judgment of Solomon. *Hum Gene Ther* **20**: 1119–1132.
11. Haralambieva, I, Iankov, I, Hasegawa, K, Harvey, M, Russell, SJ and Peng, KW (2007). Engineering oncolytic measles virus to circumvent the intracellular innate immune response. *Mol Ther* **15**: 588–597.
12. Russell, SJ and Peng, KW (2009). Measles virus for cancer therapy. *Curr Top Microbiol Immunol* **330**: 213–241.
13. Peng, KW, Ahmann, GJ, Pham, L, Greipp, PR, Cattaneo, R and Russell, SJ (2001). Systemic therapy of myeloma xenografts by an attenuated measles virus. *Blood* **98**: 2002–2007.
14. Dingli, D, Peng, KW, Harvey, ME, Greipp, PR, O'Connor, MK, Cattaneo, R *et al.* (2004). Image-guided radiovirotherapy for multiple myeloma using a recombinant measles virus expressing the thyroidal sodium iodide symporter. *Blood* **103**: 1641–1646.
15. Ong, HT, Timm, MM, Greipp, PR, Witzig, TE, Dispenzieri, A, Russell, SJ *et al.* (2006). Oncolytic measles virus targets high CD46 expression on multiple myeloma cells. *Exp Hematol* **34**: 713–720.
16. Anderson, BD, Nakamura, T, Russell, SJ and Peng, KW (2004). High CD46 receptor density determines preferential killing of tumor cells by oncolytic measles virus. *Cancer Res* **64**: 4919–4926.
17. Peng, KW, Donovan, KA, Schneider, U, Cattaneo, R, Lust, JA and Russell, SJ (2003). Oncolytic measles viruses displaying a single-chain antibody against CD38, a myeloma cell marker. *Blood* **101**: 2557–2562.
18. Nakamura, T, Peng, KW, Harvey, M, Greiner, S, Lorimer, IA, James, CD *et al.* (2005). Rescue and propagation of fully retargeted oncolytic measles viruses. *Nat Biotechnol* **23**: 209–214.
19. Hummel, HD, Kuntz, G, Russell, SJ, Nakamura, T, Greiner, A, Einsele, H *et al.* (2009). Genetically engineered attenuated measles virus specifically infects and kills primary multiple myeloma cells. *J Gen Virol* **90**(Pt 3): 693–701.

20. Pham, L, Nakamura, T, Gabriela Rosales, A, Carlson, SK, Bailey, KR, Peng, KW *et al.* (2009). Concordant activity of transgene expression cassettes inserted into E1, E3 and E4 cloning sites in the adenovirus genome. *J Gene Med* **11**: 197–206.
21. Carlson, SK, Classic, KL, Hadac, EM, Dingli, D, Bender, CE, Kemp, BJ *et al.* (2009). Quantitative molecular imaging of viral therapy for pancreatic cancer using an engineered measles virus expressing the sodium-iodide symporter reporter gene. *AJR Am J Roentgenol* **192**: 279–287.
22. Ong, HT, Hasegawa, K, Dietz, AB, Russell, SJ and Peng, KW (2007). Evaluation of T cells as carriers for systemic measles virotherapy in the presence of antiviral antibodies. *Gene Ther* **14**: 324–333.
23. Thorne, SH, Negrin, RS and Contag, CH (2006). Synergistic antitumor effects of immune cell-viral biotherapy. *Science* **311**: 1780–1784.
24. Power, AT and Bell, JC (2008). Taming the Trojan horse: optimizing dynamic carrier cell/oncolytic virus systems for cancer biotherapy. *Gene Ther* **15**: 772–779.
25. Munguia, A, Ota, T, Miest, T and Russell, SJ (2008). Cell carriers to deliver oncolytic viruses to sites of myeloma tumor growth. *Gene Ther* **15**: 797–806.
26. Esolen, LM, Ward, BJ, Moench, TR and Griffin, DE (1993). Infection of monocytes during measles. *J Infect Dis* **168**: 47–52.
27. Wurdinger, T, Badr, C, Pike, L, de Kleine, R, Weissleder, R, Breakefield, XO *et al.* (2008). A secreted luciferase for ex vivo monitoring of *in vivo* processes. *Nat Methods* **5**: 171–173.
28. Tannous, BA (2009). Gaussia luciferase reporter assay for monitoring biological processes in culture and in vivo. *Nat Protoc* **4**: 582–591.
29. Roodman, GD (2009). Pathogenesis of myeloma bone disease. *Leukemia* **23**: 435–441.
30. Power, AT and Bell, JC (2007). Cell-based delivery of oncolytic viruses: a new strategic alliance for a biological strike against cancer. *Mol Ther* **15**: 660–665.
31. Kidd, S, Spaeth, E, Dembinski, JL, Dietrich, M, Watson, K, Klopp, A *et al.* (2009). Direct evidence of mesenchymal stem cell tropism for tumor and wounding microenvironments using *in vivo* bioluminescent imaging. *Stem Cells* **27**: 2614–2623.
32. Hakkarainen, T, Särkioja, M, Lehenkari, P, Miettinen, S, Ylikomi, T, Suuronen, R *et al.* (2007). Human mesenchymal stem cells lack tumor tropism but enhance the antitumor activity of oncolytic adenoviruses in orthotopic lung and breast tumors. *Hum Gene Ther* **18**: 627–641.
33. Peng, KW, Dogan, A, Vrana, J, Liu, C, Ong, HT, Kumar, S *et al.* (2009). Tumor-associated macrophages infiltrate plasmacytomas and can serve as cell carriers for oncolytic measles virotherapy of disseminated myeloma. *Am J Hematol* **84**: 401–407.
34. Basse, PH (1995). Tissue distribution and tumor localization of effector cells in adoptive immunotherapy of cancer. *APMIS Suppl* ***55***: 1–28.
35. Read, EJ, Keenan, AM, Carter, CS, Yolles, PS and Davey, RJ (1990). *In vivo* traffic of indium-111-oxine labeled human lymphocytes collected by automated apheresis. *J Nucl Med* **31**: 999–1006.
36. Straten, P and Becker, JC (2009). Adoptive cell transfer in the treatment of metastatic melanoma. *J Invest Dermatol* **129**: 2743–2745.
37. Fisher, B, Packard, BS, Read, EJ, Carrasquillo, JA, Carter, CS, Topalian, SL *et al.* (1989). Tumor localization of adoptively transferred indium-111 labeled tumor infiltrating lymphocytes in patients with metastatic melanoma. *J Clin Oncol* **7**: 250–261.
38. Vande Broek, I, Vanderkerken, K, Van Camp, B and Van Riet, I (2008). Extravasation and homing mechanisms in multiple myeloma. *Clin Exp Metastasis* **25**: 325–334.
39. Aggarwal, R, Ghobrial, IM and Roodman, GD (2006). Chemokines in multiple myeloma. *Exp Hematol* **34**: 1289–1295.
40. Burger, JA, Ghia, P, Rosenwald, A and Caligaris-Cappio, F (2009). The microenvironment in mature B-cell malignancies: a target for new treatment strategies. *Blood* **114**: 3367–3375.
41. Kunkel, EJ and Butcher, EC (2003). Plasma-cell homing. *Nat Rev Immunol* **3**: 822–829.
42. Rajkumar, SV, Mesa, RA, Fonseca, R, Schroeder, G, Plevak, MF, Dispenzieri, A *et al.* (2002). Bone marrow angiogenesis in 400 patients with monoclonal gammopathy of undetermined significance, multiple myeloma, and primary amyloidosis. *Clin Cancer Res* **8**: 2210–2216.
43. Ong, HT, Trejo, TR, Pham, LD, Oberg, AL, Russell, SJ and Peng, KW (2009). Intravascularly administered RGD-displaying measles viruses bind to and infect neovessel endothelial cells in vivo. *Mol Ther* **17**: 1012–1021.
44. Copier, J, Ward, S and Dalgleish, A (2007). Cell based cancer vaccines: regulatory and commercial development. *Vaccine* **25**(suppl 2): B35–B46.
45. Brill, TH, Kübler, HR, Pohla, H, Buchner, A, Fend, F, Schuster, T *et al.* (2009). Therapeutic vaccination with an interleukin-2-interferon-gamma-secreting allogeneic tumor vaccine in patients with progressive castration-resistant prostate cancer: a phase I/II trial. *Hum Gene Ther* **20**: 1641–1651.
46. Buchner, A, Pohla, H, Willimsky, G, Frankenberger, B, Frank, R, Baur-Melnyk, A *et al.* (2010). Phase I trial of an allogeneic gene-modified tumor cell vaccine (RCC-26/CD80/IL-2) in patients with metastatic renal cell carcinoma. *Hum Gene Ther* (epub ahead of print).
47. Visonneau, S, Cesano, A, Porter, DL, Luger, SL, Schuchter, L, Kamoun, M *et al.* (2000). Phase I trial of TALL-104 cells in patients with refractory metastatic breast cancer. *Clin Cancer Res* ***6***: 1744–1754.
48. Cesano, A, Visonneau, S, Wolfe, JH, Jeglum, KA, Fernandez, J, Gillio, A *et al.* (1997). Toxicological and immunological evaluation of the MHC-non-restricted cytotoxic T cell line TALL-104. *Cancer Immunol Immunother* **44**: 125–136.
49. Dingli, D, Peng, KW, Harvey, ME, Vongpunsawad, S, Bergert, ER, Kyle, RA *et al.* (2005). Interaction of measles virus vectors with Auger electron emitting radioisotopes. *Biochem Biophys Res Commun* **337**: 22–29.
50. Hasegawa, K, Pham, L, O'Connor, MK, Federspiel, MJ, Russell, SJ and Peng, KW (2006). Dual therapy of ovarian cancer using measles viruses expressing carcinoembryonic antigen and sodium iodide symporter. *Clin Cancer Res* **12**: 1868–1875.
51. Badr, CE, Hewett, JW, Breakefield, XO and Tannous, BA (2007). A highly sensitive assay for monitoring the secretory pathway and ER stress. *PLoS ONE* **2**: e571.
52. Duprex, WP, McQuaid, S, Hangartner, L, Billeter, MA and Rima, BK (1999). Observation of measles virus cell-to-cell spread in astrocytoma cells by using a green fluorescent protein-expressing recombinant virus. *J Virol* **73**: 9568–9575.